Dual targeting of AKT and mammalian target of rapamycin: A potential therapeutic approach for malignant peripheral nerve sheath tumor

Changye Y. Zou,[1] Kerrington D. Smith,[1] Quan-Sheng Zhu,[1] Jun Liu,[8] Ian E. McCutcheon,[2] John M. Slopis,[3] Funda Meric-Bernstam,[1] Zhenghong Peng,[4] William G. Bornmann,[4] Gordon B. Mills,[5] Alexander J. Lazar,[6] Raphael E. Pollock,[1] and Dina Lev[7]

Departments of [1]Surgical Oncology, [2]Neurosurgery, [3]Pediatrics and Child Neurology, [4]Experimental Therapeutics, [5]Systems Biology, [6]Pathology, and [7]Cancer Biology and [8]Division of Quantitative Sciences, The University of Texas M. D. Anderson Cancer Center, Houston, Texas

Abstract

The mammalian target of rapamycin (mTOR) pathway may constitute a potential target for the treatment of malignant peripheral nerve sheath tumors (MPNST). However, investigations of other cancers suggest that mTOR blockade can paradoxically induce activation of prosurvival, protumorigenic signaling molecules, especially upstream AKT. Consequently, we hypothesized that dual phosphatidylinositol 3-kinase (PI3K)/AKT-mTOR blockade might be applicable for MPNST treatment. Expression of activated mTOR downstream targets (p4EBP1 and pS6RP) and pAKT was evaluated immunohistochemically in a tissue microarray of human MPNSTs ($n = 96$) and benign neurofibromas ($n = 31$). Results were analyzed by Wilcoxon rank-sum tests. mTOR and AKT pathways in human MPNST cell lines, and the effects of rapamycin (mTOR inhibitor), LY294002 (dual PI3K/mTOR inhibitor), and PI-103 (potent dual PI3K/AKT-mTOR inhibitor) on pathway activation were evaluated by Western blot. Effects on cell growth were evaluated via MTS and colony formation assays. Cell cycle progression and apoptosis were assessed by propidium iodide/fluorescence-activated cell sorting staining and Annexin V assays. Acridine orange staining/fluorescence-activated cell sorting analysis, electron microscopy, and Western blot evaluated autophagy induction. p4EBP1, pS6Rp, and pAKT levels were found to be significantly higher in MPNST versus neurofibroma ($P < 0.05$ for all markers). mTOR and AKT pathways were found to be highly activated in MPNST cell lines. MPNST cells were sensitive to rapamycin; however, rapamycin enhanced pAKT and peIF4E expression. PI-103 abrogated MPNST cell growth and induced G_1 cell cycle arrest potentially through repression of cyclin D1. PI-103 did not elicit apoptosis but significantly induced autophagy in MPNST cells. These results suggest further study of combined PI3K/AKT and mTOR inhibition as a novel therapy for patients harboring MPNST. [Mol Cancer Ther 2009;8(5):1157–68]

Introduction

Malignant peripheral nerve sheath tumors (MPNST) are rare spindle-cell malignancies arising proximate to peripheral nerves and thought to originate from neural crest cells, although the specific cell of origin is still uncertain (1). MPNSTs account for 3% to 10% of all soft-tissue sarcomas and are a highly aggressive histologic subtype of this heterogeneous tumor cohort (1, 2). More than half of MPNSTs occur in neurofibromatosis type 1 (NF1) patients; the remainder develop sporadically. MPNST incidence in NF1 patients is 8% to 12%, rendering this malignancy the leading cause of NF1-related mortality (3). Surgical resection represents the mainstay of MPNST therapy (1). However, because of invasive growth, propensity to metastasize, and limited sensitivity to radiation and chemotherapy, MPNST harbor a dismal prognosis. Five-year survival rates of only 20% to 50% point to an urgent need to identify and implement improved therapeutic approaches (1, 4, 5).

Recent elucidation of potential molecular events driving tumor progression have led to remarkable interest in novel, molecularly targeted therapeutic regimens. However, for this to occur in MPNST, enhanced knowledge of the pathogenesis and molecular pathobiology of this tumor is needed. Recent studies suggest that deregulation of the mammalian target of rapamycin (mTOR) is relevant in MPNST progression (6–9). Deregulation of mTOR may be partially mediated through loss of neurofibromin expression/function, the critical genetic event responsible for NF1 and therefore NF1-associated MPNST, a process also identified in sporadic MPNST (10). Neurofibromin loss results in activation of Ras and phosphatidylinositol 3-kinase (PI3K) pathways, inducing phosphorylation and inactivation of tuberin via

Received 10/23/08; revised 1/27/09; accepted 2/19/09; published OnlineFirst 5/5/09.

Grant support: Chinese Scholarship Council (C.Y. Zou), National Foundation for Cancer Research, Hope Fund seed grant (D. Lev), and National Cancer Institute Cancer Center Support Grant 5 P30 CA16672.

The costs of publication of this article were defrayed in part by the payment of page charges. This article must therefore be hereby marked *advertisement* in accordance with 18 U.S.C. Section 1734 solely to indicate this fact.

Note: Current address for C.Y. Zou: Department of Orthopedic Surgery, First Affiliated Hospital of Sun Yat-Sen University, Guangzhou, People's Republic of China 510080.

Requests for reprints: Dina Lev, Department of Cancer Biology, The University of Texas M. D. Anderson Cancer Center, 1515 Holcombe Boulevard, Unit 1104, Houston, TX 77030. Phone: 713-792-1637; Fax: 713-563-1185. E-mail: dlev@mdanderson.org

doi:10.1158/1535-7163.MCT-08-1008

AKT, leading to mTOR activation (6). mTOR functions through two separate macromolecular complexes containing either raptor (mTORC1) or rictor (mTORC2), resulting in the phosphorylation of downstream protein kinases, mainly 4E-binding proteins, S6 kinase (S6K1), and the eukaryotic elongation factor 2 for the mTORC1 complex, which are required for both ribosomal biosynthesis and translation of key mRNAs and AKT for the mTORC2 complex (11).

Evidence suggests that mTOR plays a major role in cancer progression by acting as a master switch for cellular catabolism and anabolism, enhancing cancer cell growth and proliferation (12). In addition, mTOR can induce cell cycle progression, enhance cell survival, and block cell death as dictated by the cellular context and specific downstream targets (11). Rapamycin and rapamycin derivatives that block the mTORC1 complex have been developed and are currently being evaluated in several clinical trials for a variety of hematologic and solid malignancies (13). The potential anti-MPNST effects of rapamycin and its analogues have recently been shown (6, 8, 9). MPNST cells from NF1 patients were found sensitive to rapamycin, and rapamycin could also inhibit tumor growth in genetically engineered MPNST mouse models (6). Furthermore, the rapamycin analogue RAD001 abrogated growth of human NF1-associated and sporadic MPNST cells; RAD001 treatment of human sporadic MPNST cell xenografts significantly delayed tumor growth (9). However, as shown by these studies as well as insights gleaned from other tumor systems, the effects of mTORC1 inhibitors are cytostatic rather than cytotoxic and are transient with tumor regrowth during and/or after discontinuation of treatment (6, 9).

One potential mechanism explaining this observation is the recently identified feedback loop by which mTORC1 inhibition induces activation of the protumorigenic PI3K/AKT survival pathway (14, 15). Based on these data, several studies have evaluated combined PI3K/AKT-mTOR blockade in preclinical cancer models, showing superior effects versus each inhibitor alone (16). The rationale for using combined PI3K/AKT and mTOR inhibitors for MPNST therapy is further strengthened by the suggestion that AKT is likely to be activated in MPNST due to the loss of neurofibromin (17). AKT activation potentially contributes to MPNST malignant behavior through the activation of mTOR as well as other protumorigenic downstream signaling pathways that would not be directly affected by targeting mTOR (18). Recently, dual PI3K/AKT and mTOR inhibitory compounds such as PI-103 have been developed and are being evaluated for their potential anticancer effects (19, 20). At nanomolar concentrations, PI-103 inhibits class I PI3K and also the rapamycin-sensitive mTORC1 and the rapamycin-insensitive mTORC2 complexes (20). PI-103 has recently been shown to exhibit significant antitumor activity *in vitro* and *in vivo* against several tumor types including glioma, breast, ovarian, and prostate cancers (21). However, to the best of our knowledge, this combined approach has not been previously evaluated as MPNST therapy.

In light of the above, the goals of these studies were (*a*) to examine the expression of activated mTOR downstream targets and activated AKT in a large panel of human NF1-related and sporadic MPNST specimens and cell lines, (*b*) to elucidate the potential activation of protumorigenic pathways secondary to mTOR inhibition in MPNST cells, and (*c*) to evaluate the effect of dual mTOR and AKT blockade on MPNST cell growth and survival as well as on the activation of downstream targets.

Materials and Methods

Cell Lines and Reagents

Human NF1 MPNST cell lines SNF02.2 and SNF96.2 (American Type Culture Collection), ST88-14 (a gift from Dr. Jonathan Fletcher, Brigham and Women's Hospital), and T265 (a gift from Dr. George De Vries, Hines VA Hospital) and the non-NF1 sporadic human MPNST cell line STS26T (a gift from Dr. Steven Porcelli, Albert Einstein College of Medicine) were used for our studies and maintained and propagated as described previously (22). The PI3K inhibitor LY294002, which has been shown previously to have also direct anti-mTOR effects (23), and the mTOR inhibitor rapamycin were purchased from Cayman Chemical; the dual PI3K/AKT and mTOR inhibitor PI-103 was synthesized at M. D. Anderson Cancer Center by Dr. William Bornmann. All inhibitors were dissolved as concentrated stock solutions in DMSO and stored at −80°C. When used, inhibitors were diluted with culture medium to the indicated concentrations. Commercially available antibodies were used for immunohistochemistry and/or Western blot analysis. AKT, pAKT (Ser^{473}), mTOR, pmTOR (Ser^{2448}), S6K1, pS6K1 (Thr^{398}), S6 ribosomal protein (S6RP), pS6RP (Ser^{235}/Ser^{236}), 4EBP1, p4EBP1 (Thr^{70}), eIF4E, peIF4E (Ser^{209}), pGSK-3α/β (Ser^{21}/Ser^{9}), GSK-3α/β, pMDM2 (Ser^{166}), LC3B, PTEN, and cyclin D1 were all purchased from Cell Signaling; c-Met, MDM2, BCN1, EGFR, β-actin, and anti-mouse and anti-rabbit second antibody were acquired from Santa Cruz Biotechnology.

Immunohistochemical Staining

A previously constructed human MPNST-focused tissue microarray was used for immunohistochemical staining.[9] This tissue microarray includes 121 specimens retrieved from 93 surgical procedures: 25 neurofibromas (retrieved from NF1 patients harboring MPNST) and 96 MPNST samples (55 from NF1 patients and 41 sporadic MPNSTs) representing primary (n = 33), recurrent (n = 37), or metastatic (n = 26) lesions.

Immunohistochemistry was done using 5-μm-thick tissue microarray sections as described previously (24). Briefly, paraffin sections were dewaxed and rehydrated before antigen retrieval. Endogenous peroxidase activity was quenched with 3% hydrogen peroxide in methanol before blocking with horse serum. The sectioned tissue

[9] C.Y. Zou, K. Smith, J. Liu, et al. Clinical, pathological and molecular variables predictive of malignant peripheral nerve sheath tumor (MPNST) outcome. Ann Surg, in press.

was subjected to microwave antigen retrieval. Primary antibodies described above were used. Appropriate biotinylated secondary antibodies were applied at 1:200 before ABC peroxidase system application (Vectastain ABComplex; Vector Laboratories), DAB color development (Sigma), and Mayer's hematoxylin counterstaining. Staining distribution (% positive staining cells) and intensity (0, none; 1, low; 2, intermediate; and 3, high) were evaluated and scored by two independent reviewers (K.D.S. and A.J.L., an experienced soft-tissue pathologist). For any single patient contributing more than one neurofibroma/MPNST to the tissue microarray, the lesion exhibiting higher marker expression was selected for further statistical analysis. Photographs were obtained using a Leica DM4000B microscope and a Leica HCxPL-S-APO ×40/0.75 numeric aperture objective lens (Leica Microsystems). Images were captured using SPOT digital camera (Diagnostic Instruments) and processed using SPOT advanced acquisition software (Diagnostic Instruments).

Western Blot Analysis

Western blot was done by standard methods. Briefly, 25 to 50 μg proteins extracted from cultured cells were separated by SDS-PAGE and transferred onto nitrocellulose membranes. Membranes were then blocked and blotted with relevant antibodies. Horseradish peroxidase-conjugated secondary antibodies were detected by enhanced chemiluminesence (Amersham Biosciences). IRdye680- and IRdye800-conjugated secondary antibodies (Molecular Probes) were detected using Odyssey Imaging (LICOR Biosciences).

Measurement of Cell Proliferation

Cell growth assays were done using CellTiter96 Aqueous Non-Radioactive Cell Proliferation Assay kit (Promega), per manufacturer's instructions, to evaluate the effect the different compounds, doses, and time points studied. Absorbance was measured at a wavelength of 490 nm, and the absorbance values of treated cells are presented as a percentage of the absorbance of untreated cells. Drug concentrations required to inhibit cell growth by 50% (IC_{50}) were determined by interpolation of dose-response curves.

Colony Formation Assay

MPNST cells were treated in culture dishes for 24 h with DMSO (control) and varying concentrations of PI-103. One hundred viable cells per well were replated and allowed to grow in normal medium for 10 days and then stained for 30 min at room temperature with a 6% glutaraldehyde, 0.5% crystal violet solution. Pictures were taken with a digital camera and colonies were counted.

Cell Cycle Analysis

MPNST cell monolayers were treated with relevant agents for varying periods; propidium iodide/fluorescence-activated cell sorting analysis was conducted as described previously (24).

Apoptosis Assay

Apoptosis was measured using the Apoptosis Detection Kit I (BD Biosciences) as described previously (24).

Quantification of Acidic Vesicular Organelles

Autophagy was assessed in T265 and STS26T by quantification of acidic vesicular organelles as described earlier (16). Briefly, T265 and STS26T were treated with inhibitors as above or DMSO alone. Forty-eight hours later, cells were stained with acridine orange (1 μg/mL) for 15 min (Sigma-Aldrich); samples were examined under a fluorescence microscope. For further quantification, cells were treated and stained as above, trypsinized, and analyzed via flow cytometry. Green (510-530 nm) and red (>650 nm) fluorescence emission from 2×10^4 cells illuminated with blue (488 nm) excitation light was measured using FACSCalibur (Becton Dickinson) using CellQuest software.

Electron Microscopy

STS26T and T265 cells were grown on glass coverslips and treated with PI-103 (2.5 μmol/L) or DMSO alone for 48 h and then fixed for 1 h with a solution containing 3% glutaraldehyde plus 2% paraformaldehyde in 0.1 mol/L cacodylate buffer (pH 7.3). After fixation, the samples were postfixed in 1% OsO_4 in the same buffer for 30 min and then stained with 1% uranyl acetate. Representative areas were chosen for ultrathin sectioning and electron microscopic viewing (JEM 1010 transmission electron microscope; JEOL) as described previously (16). Digital images were also obtained (AMT imaging system; Advanced Microscopy Techniques). Three replicates were done for each experiment.

Statistical Analysis

Cell culture-based assays were repeated at least three times and mean ± SD was calculated. Cell lines were examined separately. For outcomes that were measured at a single time point, two-sample t tests were used to assess the differences. Significance was set at $P \leq 0.05$. The expression of biomarkers were enumerated and calculated as average ± SD. Wilcoxon rank-sum tests were used to compare the difference in biomarkers expression between selected groups; significance was set at $P < 0.05$.

Results

AKT and mTOR Pathways Are Highly Activated in Human MPNST Tumors and Cell Lines

Previously published *in vitro* and *in vivo* studies and the enhanced understanding of NF1 loss and additional molecular events driving MPNST initiation and progression support the hypothesis that mTOR and AKT are highly activated in MPNST (6, 8, 9). However, to the best of our knowledge, the expression levels of these activated kinases in human MPNST samples have not been previously assessed. Before investigating the effect of targeted inhibitors on MPNST cells, we evaluated the activation of mTOR-regulated downstream targets (p4EBP1 and pS6RP) as well as pAKT in a recently constructed human MPNST-focused tissue microarray (24). 4EBP1 is a direct mTOR substrate; p4EBP1 positive expression was evaluated (Fig. 1A). The average of % positively stained tumor cells as well as mean intensity per group were calculated, showing a significantly higher p4EBP1 average staining distribution (%) and intensity in

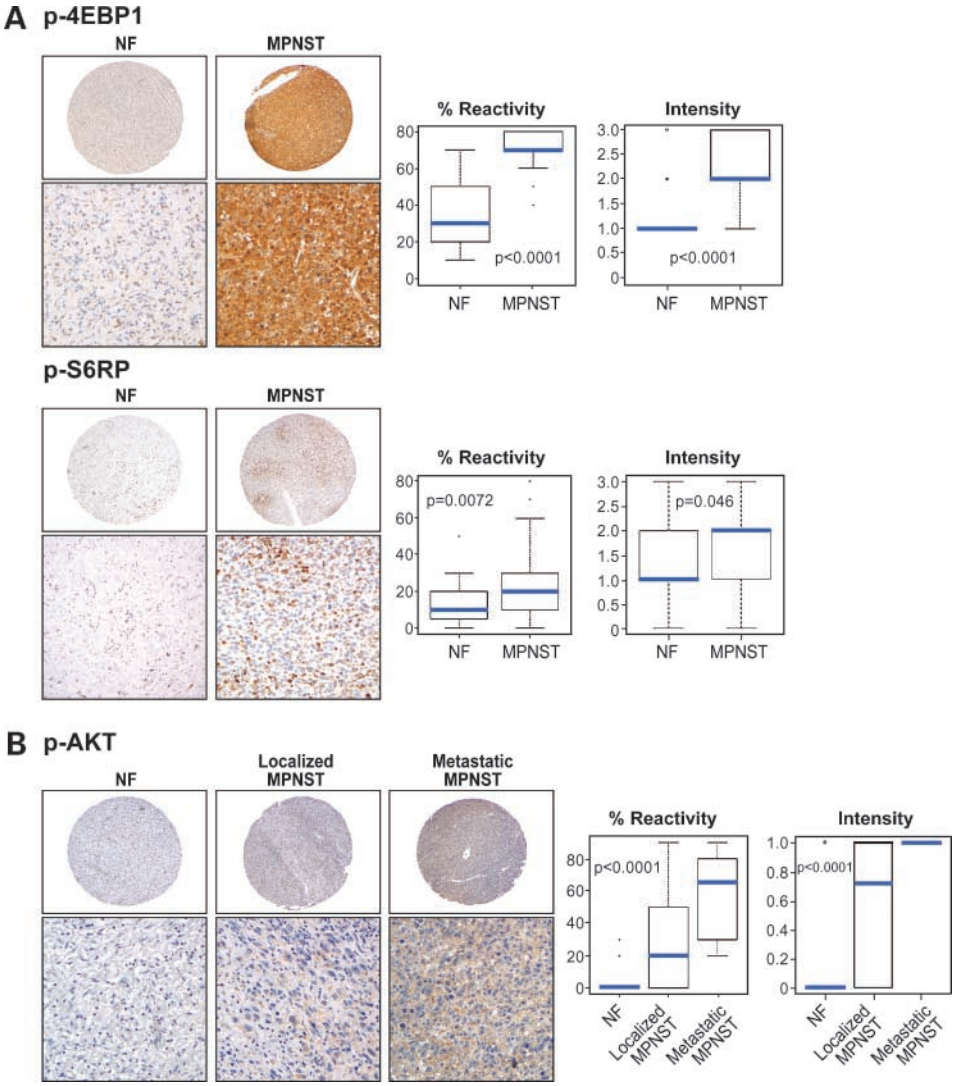

Figure 1. MPNST exhibit deregulation of the mTOR and AKT pathways. **A,** expression of activated mTOR downstream effectors 4EBP1 (*top*) and S6RP (*bottom*) in MPNST was assessed via immunohistochemistry. A tissue microarray consisting of human NF1-associated plexiform neurofibromas and NF1 associated as well as sporadic MPNST was used for immunohistochemistry. A significantly higher proportion of MPNST cells expressed p4EBP1 and pS6RP compared with neurofibromas (representative tissue microarray spots are shown; original pictures were captured at ×200). Similarly, staining intensity for both markers was significantly higher in the malignant tumors compared with the benign lesions. Results of Wilcoxon rank-sum tests: *blue line,* median of the data; *bars,* 25% and 75% quartiles; *dots,* mean outliers. The two lines are whisker lines, depicting the largest or smallest values that are not outliers. Statistical *P* values are shown. **B,** pAKT was evaluated as above; a significantly higher proportion of MPNST cells were found to exhibit a stronger pAKT expression level. Furthermore, metastatic lesions expressed higher levels of pAKT compared with localized (primary and recurrent) tumors.

MPNST compared with neurofibroma (71.9 ± 9.81% and 2.06 ± 0.71 versus 35.24 ± 16.62% and 1.19 ± 0.51 distribution and intensity in MPNST and neurofibromas, respectively; $P < 0.0001$; Fig. 1A). When MPNST was evaluated, no staining intensity differences could be seen between localized and metastatic lesions or between NF1-related and sporadic malignancies.

S6K1 is also a direct mTOR downstream target; as a surrogate marker for S6K1 activation, we evaluated the expression of pS6RP in tissue microarray samples (Fig. 1A). A significantly higher average % positive as well as mean intensity stained cells was observed in MPNST compared with neurofibromas (26.46 ± 22.57% and 1.83 ± 0.8 versus 13.74 ± 13.85% and 1.43 ± 0.66 distribution and intensity in MPNST and neurofibromas, respectively; $P = 0.0072$ and 0.046; Fig. 1A). As above, pS6RP staining intensity was not different between NF1-associated and sporadic lesions or local versus metastatic samples. These findings confirm that human MPNST exhibit a highly activated mTOR pathway. Although mTOR pathway activation could be seen to some degree in benign NF1-associated neurofibromas, the significant increase observed in MPNST suggests that additional factors acquired during malignant progression beyond the loss of neurofibromin potentially contribute to MPNST mTOR pathway activation.

We further hypothesized that AKT is highly activated in human MPNST. The expression of pAKT (Ser^{473}) was evaluated (Fig. 1B). A significantly higher average % positive as well as mean intensity stained cells was observed in MPNST compared with neurofibroma (32.54 ± 32.41% and 0.62 ± 0.48 versus 2.08 ± 7.21% and 0.04 ± 0.2 distribution and intensity in MPNST and neurofibromas, respectively; $P <$ 0.0001). Interestingly, a significantly higher pAKT % positivity and intensity expression could be identified in metastatic lesions compared with localized MPNST (59 ± 25.14% and 1 ± 0 versus 27.55 ± 31.36% and 0.55 ± 0.5 distribution and

intensity; $P < 0.0001$; Fig. 1B). No difference in pAKT expression comparing NF1-associated samples and sporadic MPNST was observed. These findings show that the PI3K/AKT pathway is highly activated in MPNST and increased activation is observed with tumor progression.

Next, we evaluated whether mTOR/AKT activation was observable in human MPNST cell lines (four NF1-associated and one sporadic) *in vitro* (Fig. 2). As shown in Fig. 2A, pmTOR and activated mTOR downstream targets (p4EBP1 and pS6K1) were shown in all cells to varying degrees; lowest pmTOR expression was seen in SNF02.2 cells corresponding to a lower expression of activated downstream targets.

In addition, we examined the expression of pAKT and its downstream substrates pGSK3β and pMDM2 (Fig. 2B); AKT pathway activation was identified in all cells to varying degree. A correlation between pAKT level and pmTOR level was shown in all of the cells excluding SNF02.2. Interestingly, this cell line expressed high pAKT levels when grown under normal culture conditions but significantly lower levels when cultured in serum-free medium (Fig. 2C). It is possible that AKT activation in this cell is highly dependent on exogenous growth factors. In comparison, a much smaller decrease in pAKT levels was observed in the other four cell lines when cultured in serum-free medium (Fig. 2C), suggesting that these cells exhibit constitutive AKT activation either due to pathway aberrations or due to autocrine growth factor loops. The AKT pathway is a common convergence point for many molecular derangements that might be occurring in MPNST including the loss of neurofibromin, overexpression and activation of numerous cell surface receptors signaling through AKT, and loss of expression/function of negative AKT regulators such as PTEN (25–28). Figure 2D shows some of the molecular alterations identified in the MPNST cells that might potentially contribute to the expression of pAKT. Data presented here support the hypothesis that the AKT and mTOR pathway are highly activated in MPNST.

Rapamycin-Mediated mTOR Blockade Inhibits MPNST Cell Growth but Induces the Activation of AKT and eIF4E

Next, we evaluated the effect of mTOR blockade via rapamycin on the growth of MPNST cells as well as downstream effectors. SNF02.2 and SNF96.2 grew extremely slowly in culture and were excluded from further studies; three MPNST cells T265, ST88, and STS26T were used. Similar to previous studies (6), a dose-dependent decrease in tumor cell growth after treatment with rapamycin (0.01-100 nmol/L/48 h) was identified (Fig. 3A). Interestingly, no additional significant effect was seen with rapamycin doses higher than 100 nmol/L (data not shown).

The effect of rapamycin on mTOR downstream signaling was evaluated in T265, ST88 (NF1-associated), and STS26T

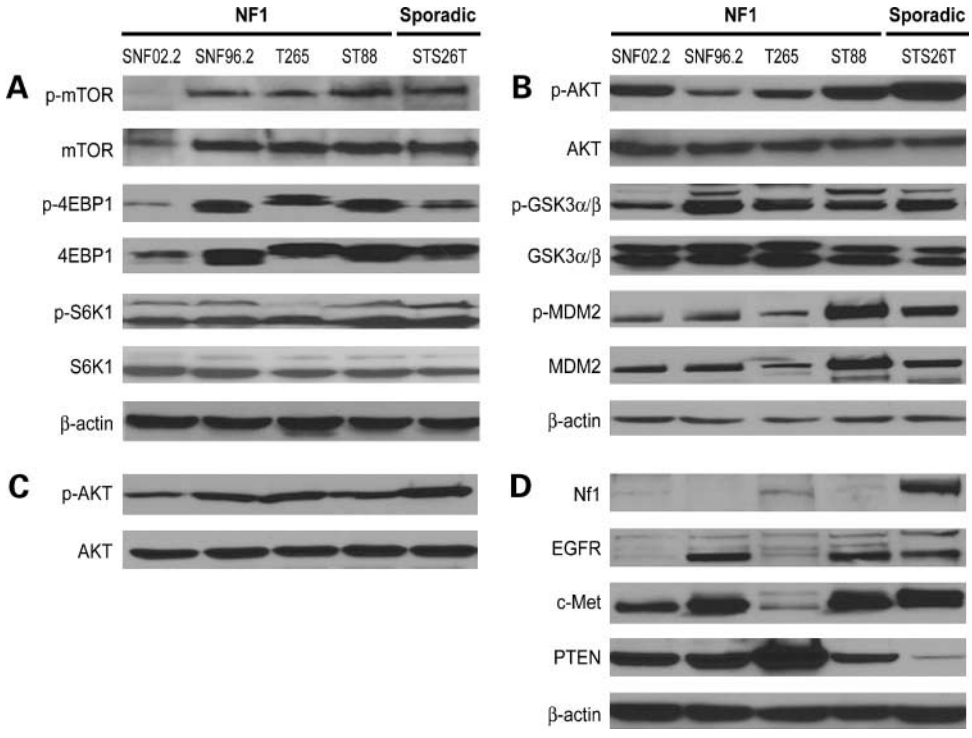

Figure 2. Human MPNST cells exhibit activated mTOR and AKT pathways. **A,** Western blots showing expression of activated mTOR and its downstream targets p4EBP1 and pS6K1 in a panel of NF1-associated (SNF02.2, SNF96.2, T265, and ST88) and sporadic (STS26T) human MPNST cell lines. **B,** activation of AKT was also found in these cells. pAKT and its downstream substrates pGSK3β and pMDM2 are expressed in MPNST cells. **C,** pAKT is expressed in MPNST cells when cultured in serum-free medium. **D,** Western blot showing expression of several possible upstream AKT modifiers in MPNST cells. *Nf1,* neurofibromin.

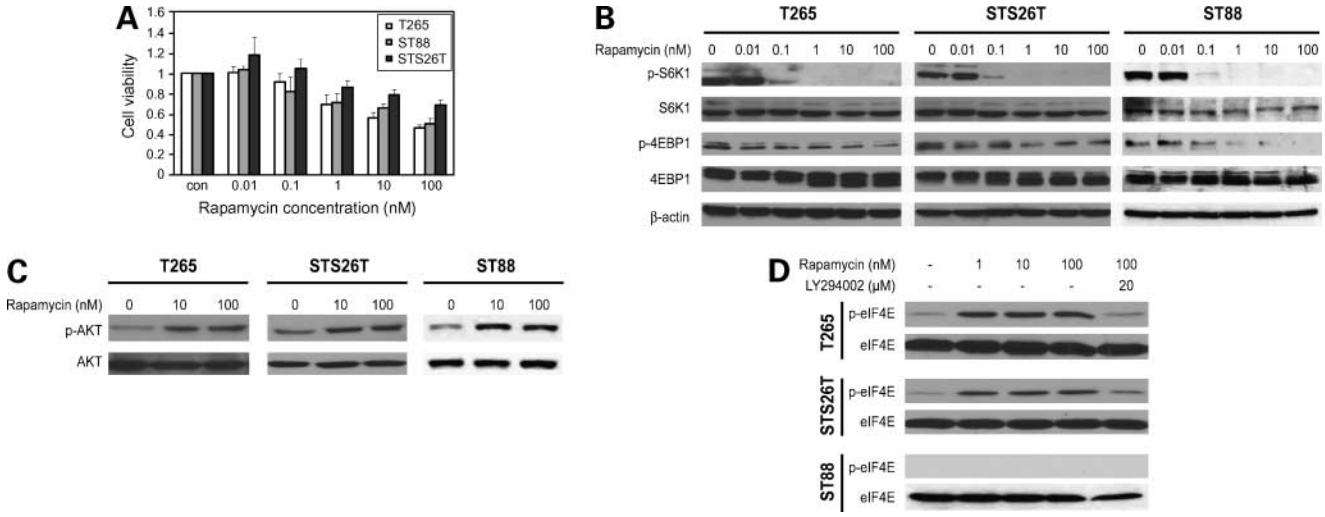

Figure 3. Rapamycin abrogates MPNST cell growth but induces the activation of AKT and eIF4E. **A,** MTS assays showing a rapamycin (48 h) dose-dependent decrease in MPNST cell growth. **B,** rapamycin (4 h) blocks the activation of the mTOR downstream targets S6K1 and 4EBP1 (Western blot). **C,** rapamycin at doses indicated induces activation of AKT in both cell lines tested (Western blot). **D,** rapamycin (4 h) induces the phosphorylation of eIF4E in MPNST cells. This activation is blocked when combining rapamycin with a PI3K inhibitor (LY294002; Western blot).

cells (sporadic MPNST). mTOR downstream target S6K1 phosphorylation was significantly decreased after exposure to 0.1 nmol/L rapamycin (4 h) and completely abolished after treatment with higher doses (Fig. 3B). Similarly, a significant decrease in 4EBP1 phosphorylation was observed (Fig. 3B). These results show potential rapamycin-induced antitumorigenic effects in human MPNST cells. However, previous studies in other tumor systems have shown that rapamycin as a single agent can also enhance unwarranted prosurvival signaling in tumor cells, especially activation of AKT, effects that might lead to therapeutic escape and resistance. To evaluate if such mechanisms are operative in MPNST, we studied the effect of rapamycin treatment on the expression of pAKT. As shown in Fig. 3C, rapamycin induced the phosphorylation of AKT in all MPNST cells tested. In addition, an increase in eIF4E phosphorylation was observed in T265 and STS26T cells (no such effect was seen in ST88 cells). Importantly, the rapamycin-induced increase in peIF4E was abolished when a PI3K inhibitor (LY294002) was concomitantly administered. The functional consequences of eIF4E phosphorylation are not well known and currently under investigation. These findings support further investigation of combined mTOR and PI3K/AKT inhibition as an anti-MPNST approach.

Combined PI3K/AKT and mTOR Inhibition Abrogate MPNST Growth and Abolishes the Potential Rapamycin-Induced Activation of Prosurvival Molecules

In the first set of experiments, we evaluated the effect of PI3K/AKT/mTOR inhibition on MPNST cell growth. A dose-dependent tumor cell growth inhibition to varying degree was observed in all three cell lines after treatment with LY294002 (1.25-20 μmol/L/48 h; Fig. 4A). In conjunction, a dose-dependent decrease in pAKT was observed after treatment with the inhibitor. pAKT inhibition in STS26T necessitated higher LY294002 doses than in T265 cells, corresponding to the sensitivity of these cells to growth inhibition by the compound (Fig. 4A). These data suggest that MPNST cells are sensitive to PI3K/AKT inhibition.

PI-103, a potent dual PI3K/AKT and mTOR inhibitor, was used to further test the combined targeting hypothesis. MPNST cell treatment with increasing PI-103 doses (0.25-4 μmol/L/48 h) induced significant growth inhibition and decreased colony formation capacity (Fig. 4B). Lower PI-103 doses were needed to achieve IC_{50} levels in MPNST cells compared with LY294002 (extrapolated IC_{50} values were PI-103 0.78 ± 0.13, 0.84 ± 0.18, and 1.56 ± 0.25 μmol/L; LY294002 3.5 ± 0.12, 9.5 ± 1.8, and 12.2 ± 2.3 μmol/L for T265, ST88, and STS26T, respectively). Similarly, a lower dose of PI-103 compared with LY294002 was needed to block AKT activation; 0.1 μmol/L/4 h PI-103 significantly reduced pAKT expression and higher doses abolished AKT phosphorylation in both T265 and STS26T cells (Fig. 4C). It is intriguing that, in contrast to LY294002, where decrease in AKT phosphorylation directly correlated with antigrowth response, low doses of PI-103 were sufficient to block AKT activation, whereas, in both cells, STS26T was less sensitive to the compound compared with T265 cells; this observation warrants further study. Most importantly, the observed reduction in pAKT, in contrast to the increased pAKT found after treatment of cells with rapamycin, reinforces the possibility of combining PI3K/AKT and mTOR inhibitors. Moreover, PI-103 significantly inhibited the mTOR pathway; dose-dependent decreases were observed in pmTOR as was inhibition of the mTOR downstream targets p706SK and its effector S6RP and also 4EBP1 (Fig. 4C). In contrast to treatment with rapamycin alone, no increase in peIF4E could be shown, and the activation of this 4EBP1 downstream effector was abolished

with PI-103 doses higher than 1 μmol/L. Taken together, these studies show that MPNST cells are highly sensitive to PI-103. Furthermore, combined PI3K/AKT and mTOR inhibition obliterates the rapamycin-induced activation of prosurvival pathways.

PI-103 Induces MPNST G_1 Cell Cycle Arrest

Data above show that PI-103 significantly inhibits the growth of MPNST cells. Consequently, we sought to evaluate the effect of this compound on MPNST cell cycle progression and apoptosis. Using propidium iodide

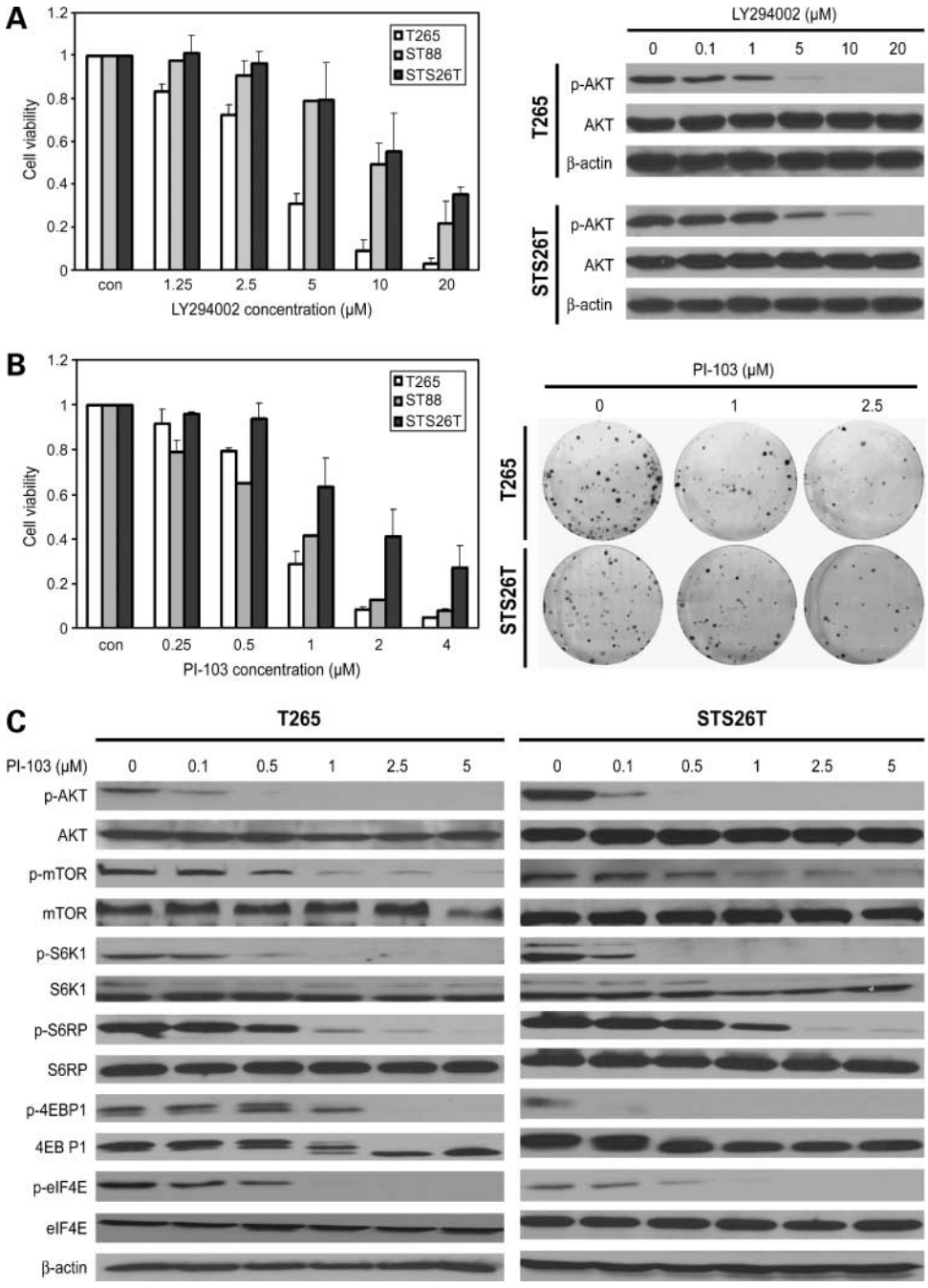

Figure 4. Dual mTOR and PI3K/AKT inhibitor PI-103 inhibits MPNST cell growth and blocks the activation of downstream targets. **A,** LY294002 (48 h) abrogates the growth of MPNST cells (MTS) and the phosphorylation of AKT in a dose-dependent manner. **B,** PI-103, a potent dual PI3K/AKT and mTOR inhibitor, abrogates the growth of MPNST cells in doses lower than those observed for LY294002 (MTS) and decreases MPNST cell colony-forming capacity. **C,** PI-103 inhibits the phosphorylation of AKT, mTOR, and its downstream targets in a dose-dependent manner (Western blot). Thus, PI-103 abrogates the induction of AKT phosphorylation seen after mTOR inhibition alone. Furthermore, in contrast to rapamycin, PI-103 treatment results in a dose-dependent decrease in eIF4E phosphorylation.

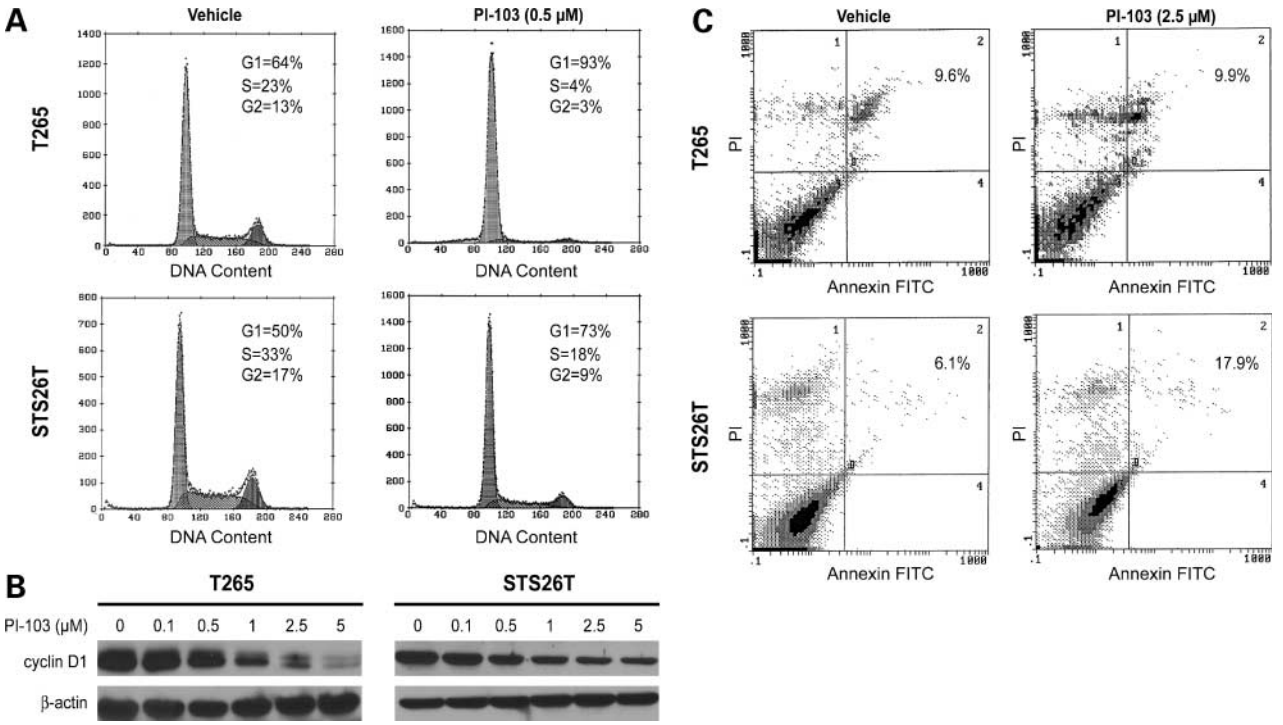

Figure 5. PI-103 induces G_1 cell cycle arrest but not apoptosis in MPNST cells. **A,** propidium iodide staining/fluorescence-activated cell sorting analysis shows G_1-phase cell cycle arrest after 48 h treatment with low-dose PI-103 (0.5 μmol/L). **B,** a PI-103 dose-dependent reduction in cyclin D1 protein expression is shown possibly contributing to the G_1 cell cycle arrest noticed above. **C,** Annexin V/fluorescence-activated cell sorting analysis show minimal MPNST cell apoptosis in response to PI-103 (2.5 μmol/L/48 h).

staining/fluorescence-activated cell sorting analysis, cell cycle distribution of MPNST cells (T265 and STS26T) treated with PI-103 (0.5 μmol/L) for 48 h was assessed. As shown in Fig. 5A, a significant G_1 cell cycle arrest was shown in both cell lines after treatment; repeat experiments showed a consistent change in MPNST cell cycle progression (G_1-phase cells in control 58.3 ± 5.8% and 49.9 ± 0.8% and PI-103 treated 86.3 ± 1.2% and 71.9 ± 2.2% for T265 and STS26T, respectively; $P < 0.05$). Concordant with this finding, a PI-103 dose-dependent decrease in cyclin D1 expression was shown (Fig. 5B), whereas no effect on p21 or p27 expression and/or localization was observed after PI-103 treatment of MPNST cells (data not shown).

The above cell cycle analyses did not show significant increases in sub-G_1 cell populations after PI-103 treatment, suggesting that PI-103 at the dose and period tested does not induce significant apoptosis in MPNST cells. To further assess apoptosis, we used an Annexin V apoptosis detection assay (Fig. 5C) using a higher PI-103 dose (2.5 μmol/L/48 h). PI-103 did not significantly increase apoptotic cell death (Fig. 5C), whereas a small increase in the necrotic cell fraction was noted (2.2 ± 0.7% and 3.2 ± 1.0% in controls versus 11.6 ± 3.2% and 14.7 ± 1.1% in treated T265 and STS26T cells, respectively).

PI-103 Induces Autophagy in Human MPNST Cells

Data above suggest that PI-103 at the doses evaluated does not induce MPNST cell death via apoptosis. Although it is possible that the PI-103-induced cell cycle arrest is the major mechanism resulting in the observed decreased cell growth, other mechanisms inducing cell death might also play a role. mTOR is known to be a major regulator of autophagy; mTOR inhibition has been shown to induce this form of cell death in cancer cells (16, 29, 30). Thus, we sought to evaluate whether PI-103 promotes autophagy in MPNST cells. The formation of acidic vesicular organelles visualized on staining with acridine orange is one of the major characteristics of autophagy. Acridine orange staining of T265 and STS26T cells showed increased acidic vesicular organelles in PI-103 (1 and 2.5 μmol/L/48 h)-treated cells compared with control DMSO-treated cells (Fig. 6A). For a quantitative analysis, MPNST cells were treated with rapamycin (100 nmol/L), LY294002 (10 μmol/L), or PI-103 (2.5 μmol/L) for 48 h; after staining with acridine orange, the cells were subjected to flow cytometric analysis. As shown in Fig. 6B, rapamycin increased acridine orange positivity (Y axis) from 4.2% and 4.8% to 21.3% and 15.1% and LY294002 increased staining to 16.1% and 14.1%, with PI-103 increasing the readout to 81.2% and 47.1% in T265 and STS26T cells, respectively, indicating the development of acidic vesicular organelles ($P < 0.05$ for all drugs compared with control and for PI-103 compared with the other two inhibitors). Electron microscopic evaluation, the gold standard for assessment of autophagy, of T265 and STS26T cells after exposure to PI-103 (2.5 μmol/L/72 h) confirmed

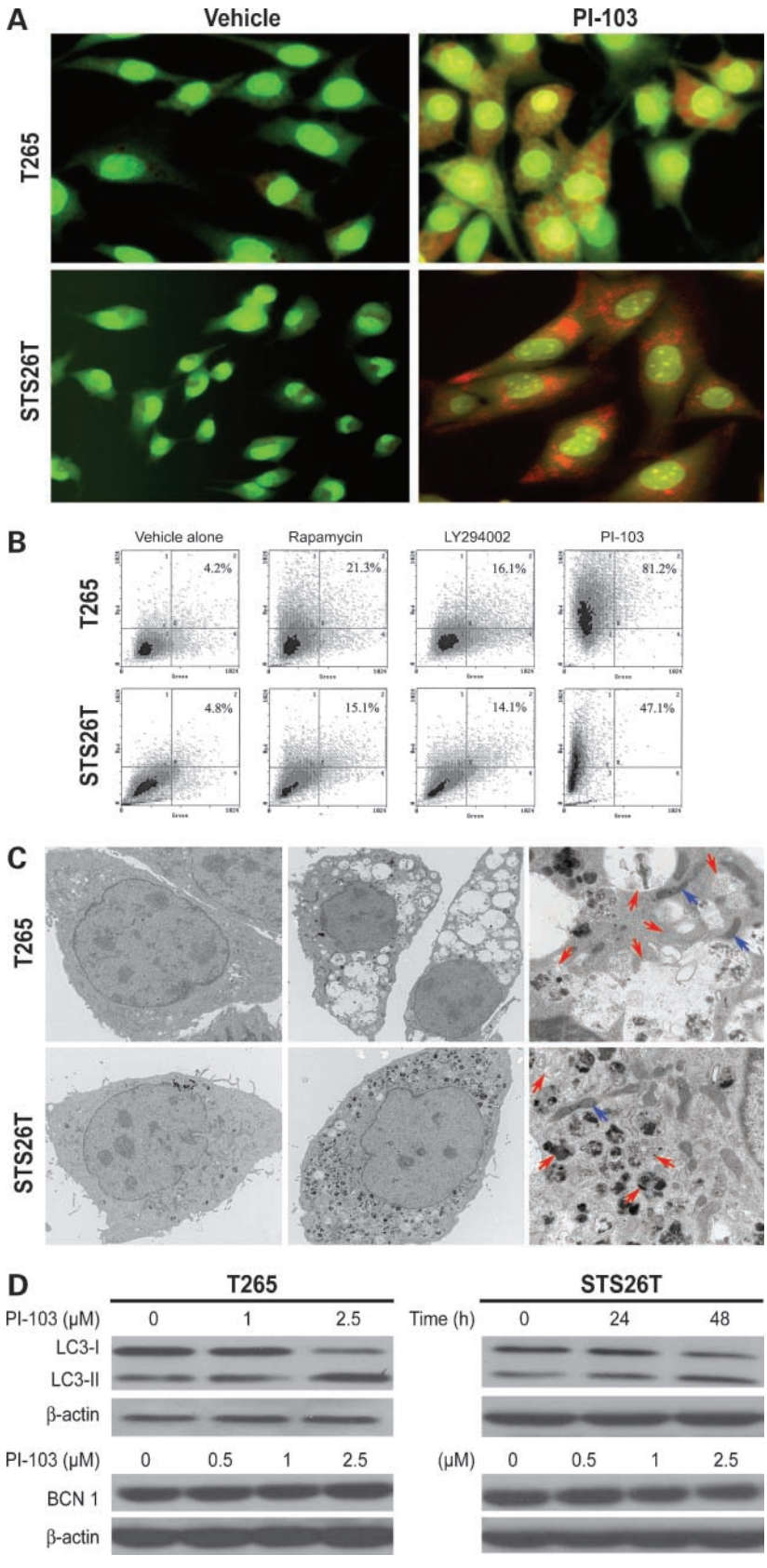

Figure 6. PI-103 induces autophagy in MPNST cells. **A,** PI-103 treatment (2.5 μmol/L/48 h) enhances the formation of autophagosomes in MPNST cells showed on acridine orange staining. **B,** MPNST cells were treated with or without rapamycin (100 nmol/L), LY294002 (10 μmol/L), or PI-103 (2.5 μmol/L) for 72 h and subjected to fluorescence-activated cell sorting analysis after acridine orange staining. % Acridine orange positive staining cells is depicted. An increase in autophagy was seen with all compounds, most significantly after treatment with PI-103 ($P < 0.05$). **C,** electron micrograph pictures showing ultrastructural changes in MPNST cells, suggesting the induction of autophagy. *Red arrowheads,* autophagic and empty vesicles; *blue arrowheads,* mitochondria (*right*). No chromatin condensation could be seen and nuclear membranes were intact, further supporting lack of apoptotic effect. **D,** Western blot showing a PI-103 dose-dependent (*top right*) and time-dependent (*top left*) increase in LC3-II in MPNST cells. *Bottom,* Western blot showing no change in beclin expression in response to PI-103.

the development of autophagy (Fig. 6C). After treatment, MPNST cells exhibited numerous autophagic and empty vesicles, indicating the massive development of autophagy without indicators of apoptosis such as chromatin condensation or fragmentation; nuclear membranes were found to be intact (Fig. 6C).

Next, LC3 expression was evaluated via Western blot. As shown in Fig. 6D, a dose- and time-dependent increase in LC3-II was observed in MPNST cells after treatment with PI-103. LC3-II is produced by cleavage of LC3 during autophagy; thus, the increase in LC3-II can be used as a marker of autophagy development (31). Due to the emerging role of beclin (ATG6) in autophagy (32), we also evaluated the effect of PI-103 on the expression of this protein. No change in beclin levels in response to PI-103 could be observed, suggesting that AKT/mTOR inhibition-induced autophagy in MPNST cells occurs independently of changes in beclin expression (Fig. 6D). Taken together, our data show that the PI3K/AKT and mTOR pathways are highly deregulated in MPNST and that a dual inhibition approach might be effective in abrogating MPNST growth and enhancing autophagy.

Discussion

In this era of personalized molecular therapies, identification of appropriate therapeutic targets is critical, especially for a disease such as MPNST, which lack efficacious treatments. mTOR has recently emerged as a potential target for the treatment of MPNST as suggested by several studies showing activation of the mTOR pathway *in vitro* and *in vivo* (6, 9). To the best of our knowledge, this report is the first to confirm mTOR pathway activation in a relatively large cohort of human MPNST specimens, further supporting investigation of treatment approaches that target this pathway. Moreover, significant AKT pathway activation was also shown to increase with MPNST progression, exhibiting highest levels in metastatic lesions. mTOR is a downstream target of AKT; however, other mTOR-independent signaling molecules are also affected by AKT activation and these could also contribute to MPNST tumorigenicity and metastasis. Our results suggest that, in addition to mTOR, AKT activation blockade either by inhibition of the PI3K upstream or directly through AKT inhibitors should also be potentially pursued as a systemic anti-MPNST approach. Interestingly, NF1-positive MPNST samples expressed significantly higher levels of activated mTOR/AKT compared with plexiform neurofibromas, although the latter also exhibit loss of neurofibromin. These findings suggest that, whereas neurofibromin loss might contribute to AKT/mTOR deregulation, other molecular derangements acquired throughout the tumorigenic process may also be relevant. For example, among other potential mechanisms, overexpression and activation of the EGFR and c-Met tyrosine kinase receptors as well as loss of PTEN expression have been identified in MPNST (25–28, 33–36). No difference in AKT/mTOR activation could be identified when we compared NF1-associated and sporadic MPNST samples. It has been shown previously that some sporadic MPNSTs also exhibit loss of neurofibromin function (10), and it is possible the same molecular aberrations contributing to NF1-associated MPNST are important in sporadic lesions as well.

Accumulating evidence from a variety of cancer types implicate the mTOR pathway in tumorigenesis, tumor progression, angiogenesis, metastasis, and chemotherapy resistance (11, 13). These findings have led to development of various mTOR inhibitors currently being evaluated in preclinical models and clinical trials (37). Similar to previously published data, our results show that MPNST cells are sensitive to mTOR blockade (6). However, intensive mTOR-focused research has identified that mTOR inhibition by rapamycin or its analogues can result in paradoxical effects by which mTOR blockade leads to enhanced activation of AKT, resulting in the elevation of cell survival signals (14, 15, 38). This effect is potentially mediated via inhibition of the mTOR downstream target S6K1, which, on activation, indirectly represses AKT phosphorylation (15). In addition, rapalogs are thought to disrupt the assembly of mTORC1 but generally spare mTORC2 (39). Inhibition of mTORC1 could promote the assembly of mTORC2 following the interaction of mTOR with rictor and mSin1; as mTORC2 phosphorylates AKT Ser^{473}, activation of mTORC2 might counteract the antitumor activity of contemporary mTOR inhibitors (40). Rapamycin-induced AKT phosphorylation has been identified to be tumor-specific and cell type-specific (41); our results show that AKT activation does occur in MPNST cells in response to rapamycin. Furthermore, we showed that rapamycin induces the phosphorylation of eIF4E in some MPNST cells. eIF4E, an indirect target of mTOR through phosphorylation of 4EBP1, has been shown previously to enhance the expression of proteins involved in cell growth, survival, and angiogenesis (42), is overexpressed in a variety of human malignancies, and is thought to play a major role in cancer progression (43). The functional effect of eIF4E phosphorylation is not fully understood; in several investigative models, phosphorylation (at Ser^{209}) was found to enhance eIF4E affinity to the cap structures and increase its translational activity (14). Collectively, these potential unwarranted effects of rapamycin in MPNST cells decrease the appeal of mTOR inhibitors as single agents for MPNST treatment and point to a potential benefit of combinatorial approaches.

Based on the above and the finding that AKT is highly activated in MPNST, it is possible that AKT blockade alone and/or in combination with other modalities might have significant effect on MPNST growth and metastasis and should be further explored. Specifically pertaining to our studies, combined inhibition of AKT and mTOR could be very effective as an anti-MPNST therapy. In recent years, efforts have been made to identify and develop kinase inhibitors that target several molecular targets within a single type of cancer or patient. Dual PI3K/AKT and mTOR inhibitors are currently under development and testing. PI-103 is one potential compound, which has shown efficacy in several preclinical tumor models (20, 21, 44). Our results show that MPNST cells are highly sensitive to PI-103. This compound

has been shown to abolish the effect of rapamycin on AKT and eIF4E in MPNST cells potentially through the direct effect of PI-103 on PI3K as well as through its identified ability to block mTORC2 in addition to mTORC1 (20).

p53 mutations are common in MPNST and p53 deregulation may be of major relevance to MPNST progression (45, 46). STS26T cells were previously identified to be null for p53 (22). Thus, it is possible that PI-103 inhibits MPNST cell growth and induces MPNST G_1 cell cycle arrest in a p53 status-independent manner, a finding of major clinical importance. A p53 status-independent mTOR blockade-induced G_1 cell cycle arrest has been previously shown in other tumor systems (47). We observed that PI-103 induced autophagy in MPNST, an effect that was significantly more robust than after treatment with a mTOR inhibitor (rapamycin) or the less potent PI3K/mTOR inhibitor, LY294002. mTOR is a major regulator of cell survival, and rapamycin has been previously identified to induce apoptosis as well as autophagy (47). Similarly, pAKT has been shown to induce antiapoptotic as well as antiautophagic effects (48). LY294004 was initially shown to inhibit autophagy in normal cells possibly through its effect on class III PI3K (49). However, recent data show that LY294002 induces autophagy in glioma cells, at least in part, by inhibiting AKT activity (16). Combined PI3K and mTOR inhibition did not elicit MPNST cell apoptosis but instead resulted in significant autophagy, and it is possible that this autophagy per se leads to MPNST cell death. The mechanisms resulting in PI-103-induced autophagy and its function are currently unknown, and studies of this process are ongoing.

In summary, our investigations show that human MPNST exhibit both AKT and mTOR deregulation and show the inhibitory effect of dual PI3K/AKT and mTOR blockade on MPNST cell growth, thereby providing a strong rationale for considering this combined approach for treatment of patients burdened by MPNST.

Disclosure of Potential Conflicts of Interest

No potential conflicts of interest were disclosed.

Acknowledgments

We thank the Chinese Scholarship Council and the National Foundation for Cancer Research (Hope Fund) for partial financial support of the studies, Kenneth Dunner for assistance with electron microscopy, and Kim Vu for aid in figure preparation.

References

1. Ducatman BS, Scheithauer BW, Piepgras DG, Reiman HM, Ilstrup DM. Malignant peripheral nerve sheath tumors. A clinicopathologic study of 120 cases. Cancer 1986;57:2006–21.

2. Collin C, Godbold J, Hajdu S, Brennan M. Localized extremity soft tissue sarcoma: an analysis of factors affecting survival. J Clin Oncol 1987; 5:601–12.

3. Evans DG, Baser ME, McGaughran J, Sharif S, Howard E, Moran A. Malignant peripheral nerve sheath tumours in neurofibromatosis 1. J Med Genet 2002;39:311–4.

4. Anghileri M, Miceli R, Fiore M, et al. Malignant peripheral nerve sheath tumors: prognostic factors and survival in a series of patients treated at a single institution. Cancer 2006;107:1065–74.

5. Wong WW, Hirose T, Scheithauer BW, Schild SE, Gunderson LL. Malignant peripheral nerve sheath tumor: analysis of treatment outcome. Int J Radiat Oncol Biol Phys 1998;42:351–60.

6. Johannessen CM, Reczek EE, James MF, Brems H, Legius E, Cichowski K. The NF1 tumor suppressor critically regulates TSC2 and mTOR. Proc Natl Acad Sci U S A 2005;102:8573–8.

7. Dasgupta B, Yi Y, Chen DY, Weber JD, Gutmann DH. Proteomic analysis reveals hyperactivation of the mammalian target of rapamycin pathway in neurofibromatosis 1-associated human and mouse brain tumors. Cancer Res 2005;65:2755–60.

8. Johannessen CM, Johnson BW, Williams SM, et al. TORC1 is essential for NF1-associated malignancies. Curr Biol 2008;18:56–62.

9. Johansson G, Mahller YY, Collins MH, et al. Effective in vivo targeting of the mammalian target of rapamycin pathway in malignant peripheral nerve sheath tumors. Mol Cancer Ther 2008;7:1237–45.

10. Perry A, Roth KA, Banerjee R, Fuller CE, Gutmann DH. NF1 deletions in S-100 protein-positive and negative cells of sporadic and neurofibromatosis 1 (NF1)-associated plexiform neurofibromas and malignant peripheral nerve sheath tumors. Am J Pathol 2001;159:57–61.

11. Guertin DA, Sabatini DM. An expanding role for mTOR in cancer. Trends Mol Med 2005;11:353–61.

12. Abraham RT. Identification of TOR signaling complexes: more TORC for the cell growth engine. Cell 2002;111:9–12.

13. Sabatini DM. mTOR and cancer: insights into a complex relationship. Nat Rev Cancer 2006;6:729–34.

14. Sun SY, Rosenberg LM, Wang X, et al. Activation of Akt and eIF4E survival pathways by rapamycin-mediated mammalian target of rapamycin inhibition. Cancer Res 2005;65:7052–8.

15. Wan X, Harkavy B, Shen N, Grohar P, Helman LJ. Rapamycin induces feedback activation of Akt signaling through an IGF-1R-dependent mechanism. Oncogene 2007;26:1932–40.

16. Takeuchi H, Kondo Y, Fujiwara K, et al. Synergistic augmentation of rapamycin-induced autophagy in malignant glioma cells by phosphatidylinositol 3-kinase/protein kinase B inhibitors. Cancer Res 2005;65: 3336–46.

17. Cichowski K, Santiago S, Jardim M, Johnson BW, Jacks T. Dynamic regulation of the Ras pathway via proteolysis of the NF1 tumor suppressor. Genes Dev 2003;17:449–54.

18. Tokunaga E, Oki E, Egashira A, et al. Deregulation of the Akt pathway in human cancer. Curr Cancer Drug Targets 2008;8:27–36.

19. Knight ZA, Gonzalez B, Feldman ME, et al. A pharmacological map of the PI3-K family defines a role for p110α in insulin signaling. Cell 2006; 125:733–47.

20. Fan QW, Knight ZA, Goldenberg DD, et al. A dual PI3 kinase/mTOR inhibitor reveals emergent efficacy in glioma. Cancer Cell 2006;9: 341–9.

21. Raynaud FI, Eccles S, Clarke PA, et al. Pharmacologic characterization of a potent inhibitor of class I phosphatidylinositide 3-kinases. Cancer Res 2007;67:5840–50.

22. Miller SJ, Rangwala F, Williams J, et al. Large-scale molecular comparison of human Schwann cells to malignant peripheral nerve sheath tumor cell lines and tissues. Cancer Res 2006;66:2584–91.

23. Brunn GJ, Williams J, Sabers C, Wiederrecht G, Lawrence JC, Jr., Abraham RT. Direct inhibition of the signaling functions of the mammalian target of rapamycin by the phosphoinositide 3-kinase inhibitors, wortmannin and LY294002. EMBO J 1996;15:5256–67.

24. Zhu QS, Ren W, Korchin B, et al. Soft tissue sarcoma cells are highly sensitive to AKT blockade: a role for p53-independent up-regulation of GADD45α. Cancer Res 2008;68:2895–903.

25. Holtkamp N, Malzer E, Zietsch J, et al. EGFR and erbB2 in malignant peripheral nerve sheath tumors and implications for targeted therapy. Neuro Oncol 2008;10:946–57.

26. Mawrin C, Kirches E, Boltze C, Dietzmann K, Roessner A, Schneider-Stock R. Immunohistochemical and molecular analysis of p53, RB, and PTEN in malignant peripheral nerve sheath tumors. Virchows Arch 2002;440:610–5.

27. Kawaguchi K, Oda Y, Saito T, et al. Genetic and epigenetic alterations of the PTEN gene in soft tissue sarcomas. Hum Pathol 2005;36:357–63.

28. Kawaguchi K, Oda Y, Saito T, et al. DNA hypermethylation status of multiple genes in soft tissue sarcomas. Mod Pathol 2006;19: 106–14.

29. Kanazawa T, Taneike I, Akaishi R, et al. Amino acids and insulin control autophagic proteolysis through different signaling pathways in relation to mTOR in isolated rat hepatocytes. J Biol Chem 2004;279:8452–9.

30. Iwamaru A, Kondo Y, Iwado E, et al. Silencing mammalian target of rapamycin signaling by small interfering RNA enhances rapamycin-induced autophagy in malignant glioma cells. Oncogene 2007;26:1840–51.

31. Tanida I, Minematsu-Ikeguchi N, Ueno T, Kominami E. Lysosomal turnover, but not a cellular level, of endogenous LC3 is a marker for autophagy. Autophagy 2005;1:84–91.

32. Liang XH, Jackson S, Seaman M, et al. Induction of autophagy and inhibition of tumorigenesis by beclin 1. Nature 1999;402:672–6.

33. Li H, Velasco-Miguel S, Vass WC, Parada LF, DeClue JE. Epidermal growth factor receptor signaling pathways are associated with tumorigenesis in the Nf1:p53 mouse tumor model. Cancer Res 2002;62:4507–13.

34. Ling BC, Wu J, Miller SJ, et al. Role for the epidermal growth factor receptor in neurofibromatosis-related peripheral nerve tumorigenesis. Cancer Cell 2005;7:65–75.

35. Tabone-Eglinger S, Bahleda R, Cote JF, et al. Frequent EGFR positivity and overexpression in high-grade areas of human MPNSTs. Sarcoma 2008;2008:849156.

36. Mantripragada KK, Spurlock G, Kluwe L, et al. High-resolution DNA copy number profiling of malignant peripheral nerve sheath tumors using targeted microarray-based comparative genomic hybridization. Clin Cancer Res 2008;14:1015–24.

37. Wan X, Helman LJ. The biology behind mTOR inhibition in sarcoma. Oncologist 2007;12:1007–18.

38. Wang X, Yue P, Chan CB, et al. Inhibition of mammalian target of rapamycin induces phosphatidylinositol 3-kinase-dependent and Mnk-mediated eukaryotic translation initiation factor 4E phosphorylation. Mol Cell Biol 2007;27:7405–13.

39. Loewith R, Jacinto E, Wullschleger S, et al. Two TOR complexes, only one of which is rapamycin sensitive, have distinct roles in cell growth control. Mol Cell 2002;10:457–68.

40. Sarbassov DD, Guertin DA, Ali SM, Sabatini DM. Phosphorylation and regulation of Akt/PKB by the rictor-mTOR complex. Science 2005;307:1098–101.

41. Sarbassov DD, Ali SM, Sengupta S, et al. Prolonged rapamycin treatment inhibits mTORC2 assembly and Akt/PKB. Mol Cell 2006;22:159–68.

42. Fingar DC, Salama S, Tsou C, Harlow E, Blenis J. Mammalian cell size is controlled by mTOR and its downstream targets S6K1 and 4EBP1/eIF4E. Genes Dev 2002;16:1472–87.

43. Larsson O, Li S, Issaenko OA, et al. Eukaryotic translation initiation factor 4E induced progression of primary human mammary epithelial cells along the cancer pathway is associated with targeted translational deregulation of oncogenic drivers and inhibitors. Cancer Res 2007;67:6814–24.

44. Kojima K, Shimanuki M, Shikami M, et al. The dual PI3 kinase/mTOR inhibitor PI-103 prevents p53 induction by Mdm2 inhibition but enhances p53-mediated mitochondrial apoptosis in p53 wild-type AML. Leukemia 2008;22:1728–36.

45. Birindelli S, Perrone F, Oggionni M, et al. Rb and TP53 pathway alterations in sporadic and NF1-related malignant peripheral nerve sheath tumors. Lab Invest 2001;81:833–44.

46. Cichowski K, Shih TS, Schmitt E, et al. Mouse models of tumor development in neurofibromatosis type 1. Science 1999;286:2172–6.

47. Hosoi H, Dilling MB, Shikata T, et al. Rapamycin causes poorly reversible inhibition of mTOR and induces p53-independent apoptosis in human rhabdomyosarcoma cells. Cancer Res 1999;59:886–94.

48. Pene F, Claessens YE, Muller O, et al. Role of the phosphatidylinositol 3-kinase/Akt and mTOR/P70S6-kinase pathways in the proliferation and apoptosis in multiple myeloma. Oncogene 2002;21:6587–97.

49. Aki T, Yamaguchi K, Fujimiya T, Mizukami Y. Phosphoinositide 3-kinase accelerates autophagic cell death during glucose deprivation in the rat cardiomyocyte-derived cell line H9c2. Oncogene 2003;22:8529–35.